available at www.sciencedirect.com
journal homepage: www.europeanurology.com

European Association of Urology

Prostate Cancer

Role of Dynamic Contrast-Enhanced Magnetic Resonance (MR) Imaging and Proton MR Spectroscopic Imaging in the Detection of Local Recurrence after Radical Prostatectomy for Prostate Cancer

Alessandro Sciarra [a,*], *Valeria Panebianco* [b], *Stefano Salciccia* [a], *Marcello Osimani* [b], *Danilo Lisi* [b], *Mauro Ciccariello* [b], *Roberto Passariello* [b], *Franco Di Silverio* [a], *Vincenzo Gentile* [a]

[a] *Department of Urology, University Sapienza, Rome, Italy*
[b] *Department of Radiology, University Sapienza, Rome, Italy*

Article info

Article history:
Accepted December 14, 2007
Published online ahead of print on December 31, 2007

Keywords:
Prostate cancer
Radical prostatectomy
Spectroscopy
Magnetic resonance

Abstract

Objectives: To assess the accuracy of magnetic resonance (MR) spectroscopic imaging (1H-MRSI) and dynamic contrast-enhanced MR (DCEMR) in the depiction of local prostate cancer recurrence in patients with biochemical progression after radical prostatectomy (RP).

Materials and methods: 1H-MRSI and DCEMR were performed in 70 patients at high risk of local recurrence after RP. The population was divided on the basis of the clinical validation of MR results with the use of a transrectal ultrasound biopsy examination in a group of 50 patients (group A) and the prostate-specific antigen (PSA) serum level restitution after external beam radiotherapy, in a group of 20 patients (group B).

Results: In group A, 1H-MRSI analysis alone showed a sensitivity of 84% and a specificity of 88%; the DCEMR analysis alone, a sensitivity of 71% and a specificity of 94%; combined 1HMRSI-DCEMR, a sensitivity of 87% and specificity of 94%. Areas under the receiver operating characteristic (ROC) curve for 1HMRSI, DCEMR, and combined 1HMRSI /DCEMR were 0.942, 0.93,1 and 0.964, respectively.

In group B, 1HMRSI alone showed a sensitivity of 71% and a specificity of 83%; DCEMR, a sensitivity of 79% and a specificity of 100%; combined 1HMRSI and DCEMR, a sensitivity of 86% and a specificity of 100%. Areas under the ROC curve for each of these groups were 0.81, 0.923, and 0.94, respectively.

Conclusion: Our results show that combined 1H-MRSI and DCMRE is an accurate method to identify local prostate cancer recurrence in patients with biochemical progression after RP.

* Corresponding author. Department of Urology, University Sapienza, Viale Policlinico 155, Rome, Italy.
E-mail address: sciarrajr@hotmail.com (A. Sciarra).

1. Introduction

At present, tumor recurrence or progression after radical prostatectomy (RP) is assessed by prostate-specific antigen (PSA) serum level measurements and pathological findings of the tumor [1,2]. In particular, a PSA increase over a threshold of 0.2 ng/ml later than 6–12 mo following RP suggests treatment failure with a high risk of local recurrence [3,4], whereas a PSA increase within a shorter period strongly correlates with the presence of distant metastasis progression [5]. In patients with biochemical failure after RP, a diagnostic imaging procedure is often performed to distinguish between local cancer recurrence and distant spread of disease [6,7]. This information influences further therapeutic decisions. Computed tomography (CT) imaging is not widely used for the detection of local recurrence because of the low accuracy of this technique in the differentiation of post-RP local recurrence from postsurgical scarring [8]. Immunoscintigraphy [9] and carbon11 choline positron emission tomography-computed tomography [10] have been introduced as innovative imaging modalities for the detection of disease relapse, but their role is still incompletely defined. Transrectal ultrasound (TRUS) in combination with a TRUS-guided biopsy of the prostatic fossa is considered the most accurate postprostatectomy method to detect local cancer recurrence [11]. However, in the early phase of relapse, when cancer volume is low, Saleem et al [12] have shown that almost 30% of patients have biopsy-proven local recurrence if serum PSA level is <1 ng/ml and that no positive biopsy was found in patients with PSA <0.5 ng/ml. Other studies have reported that the higher serum PSA level after RP is correlated with a higher positive biopsy rate [13,14].

The efficacy of radiotherapy in the treatment of patients with low-volume local recurrences validates the importance of developing a diagnostic technique to detect early post-RP cancer recurrence [15]. Several studies have shown that MR imaging possesses high-contrast and spatial resolution, and may represent a promising technique for accurate evaluation of patients with biochemical relapse after RP [16]. A large number of studies [17,18] have shown that combined 1H-spectroscopic imaging (1H-MRSI) and dynamic contrast-enhanced MR imaging (DCEMR) could represent a powerful tool for the initial detection of prostate cancer, and for the early diagnosis of postoperative recurrence [19–22]. However, to our knowledge, no prior study has evaluated the sensitivity and specificity of 1H-MRSI and DCEMR individually and in combination in the detection of prostate cancer local recurrence after RP. Therefore, the purpose of this study was to perform this analysis in a group of patients with biopsy-proven cancer recurrence and in a second group with reduction in PSA level ($>50\%$) following radiation therapy in whom a TRUS biopsy is difficult to perform because of the low volume of the suspected locoregional cancer.

2. Materials and methods

2.1. Study approval and patient population

The protocol was approved by the local ethics committee and all subjects gave written informed consent before inclusion in the study. Between January 2006 and May 2007, we included in the study 70 consecutive male patients who were at high risk for local cancer recurrence after RP on the basis of the pathological stage and postoperative PSA increase, and who were candidates for external beam radiotherapy. All patients were submitted to RP in the urological department of our university. Patients' age at the time of diagnosis ranged between 56 and 72 yr (mean, 63.8). Inclusion criteria and clinical information gathered for each patient included a surgical pathological local stage pT3a-b; negative surgical margins; post-RP PSA increase >0.2 ng/ml (Hybritech method) later than 6 mo after surgery (mean, 13 ± 4 mo); no adjuvant or neoadjuvant hormone therapies; negative regional lymph nodes (pN0); and no evidence of distant metastases at CT scan and bone scan performed before RP. A control group (CG) of 10 postprostectomy patients with no suspicion of recurrence or progression (pT2–pN0–M0 with post-RP PSA levels <0.2 ng/ml) were also evaluated for comparison.

All patients at biochemical progression were also submitted to abdomen-pelvic TC and bone scintigraphy to excluded clinical progression.

2.2. MR equipment and image acquisition protocol

All 80 cases were examined after RP (at PSA progression for the 70 cases at high risk of local recurrence and at 6 mo after surgery for the 10 cases in the CG) with the use of a commercially available 1.5-T scanner (Magnetom Avanto, Siemens Medical Solutions, Erlangen, Germany; gradient strength, 45 mT/m; slew rate, 346 T/m/s; rise time, 400 micro/s; featuring total imaging matrix-TIM® technology), equipped with surface phased array (Body Matrix, Siemens Medical Solutions) and endorectal coil, filled with 70–90 ml of air on the basis of patient tolerance (e-Coil, Medrad, Pittsburgh, PA, USA, combined with Endo-Interface, Siemens Medical Solutions). Morphological imaging of the postprostatectomy fossa was performed by acquiring turbo spin echo (TSE) T2-weighted sequences in the axial, sagittal, and coronal planes, with the use of optimized parameters for a better spatial resolution (repetition time [TR], 5190 ms; echo time [TE], 95 ms; flip angle, 150°; average, 3; field of view (FOV) read, 256 mm; FOV phase, 100; thickness, 3 mm; section gap, 0; matrix, 512×512; phase resolution, 100%; band width, 130; scan time, 3.40 min). 1H-MRSI data were acquired by two

expert radiologists (V.P. and M.C.) after a first review of morphological images, with maximizing of the coverage of the selected region of suspect recurrence, whereas reducing the inclusion of surrounding structures (muscles, fat, rectal air, urine). In patients with hypointense areas suspected for disease recurrence on morphological images, the volume of interest (VOI) was focused on these regions; in the control group and in patients with no morphological evidence of disease recurrence, the VOI was focused on the periurethral-perianastomotic region. 1H-MRSI was performed by using a section-selected box drawn closely around the prostate fossa, and a point-resolved spectroscopic sequence was obtained with the use of three-dimensional (3D) chemical shift imaging (CSI) sequence with spectral/spatial pulses optimized for quantitative detection of choline and citrate.

DCEMR images were acquired by using a 3D, fast low-angle shot (FLASH), T1-weighted spoiled gradient-echo sequence (TR, 2.44 ms; TE, 0.9 ms; flip angle, 30°; average, 1; thickness, 4 mm; section gap, 0; section number, 12; matrix, 256 × 256; phase resolution, 100%; band width, 120; TA, 4.40 min) to perform 10 measurements in rapid succession, immediately following completion of an intravenous bolus injection of 0.1 mmol of gadopentetate dimeglumine (Multihance, Bracco Spa, Milano, Italy). Contrast was administered with a power injector (Spectris, Medrad) at 2.5 ml/s and was followed by a 15-ml saline flush. Total acquisition time for dynamic contrast-enhanced images was approximately 5 min (6–10 images per second). The 3D volume was acquired with the same positioning angle and center as the transverse T2-weighted sequence covering the entire prostate fossa and the periurethral-perianastomotic region. Relative gadolinium chelate concentration curves were calculated.

2.3. MR images and data analysis

All 80 cases were submitted to this MR protocol and, in all cases, MR images were analyzed in consensus by two radiologists (V.P. and M.C.) with long experience in urogenital magnetic resonance imaging (MRI), who used an off-line console (Leonardo, Siemens Medical Solutions, Erlangen, Germany). They were unaware of initial PSA serum levels, TRUS biopsy results, or PSA level after radiation therapy. On T2-weighted images, suspicious areas of low intensity within a high-intensity zone (ie, fat tissue) were evaluated for localization, size, morphology, signal intensity, and invasion of adjacent structures by soft tissue in the prostate fossa. An operator-independent standard postprocessing protocol, using a dedicated software (Syngo Spectroscopy Evaluation) for spectroscopic analysis, was applied to the 1H-MRSI data. Data sets were acquired as a 16 × 8 × 8 phase-encoded matrix before Fourier transformation into the spatial dimensions. This transformation resulted in spectroscopic measurements of 1024 voxels for patient with a nominal spectral and spatial resolution $> 0.3\ cm^3$. Average postprocessing duration was 25–30 min for each data set. The software (Syngo Spectroscopy Evaluation) analyzed resonance areas using an automatic Gaussian curve and revealed irregular regions of interest (ROIs). Voxels that showed substantial lipid contamination or spectral signal-to-noise ratio lower than 3:1 were rejected: This protocol for image analysis was used to reduce MRSI final data contamination by field inhomogeneity or susceptibility

The dynamic MR postprocessing procedure was performed in 10 min per patient by an MR radiologist (V.P.) with 7 yr experience. Functional dynamic imaging parameters were estimated as follows: Each MR signal enhancement-time curve was compared with a pelvic reference (pelvic muscle) before contrast material injection for each patient. Consequently, the enhancement curve was modeled with four parameters: onset time of signal enhancement, time to peak (TTP), peak enhancement, and washout. This technique has been previously described [22].

2.4. Evaluation of MR images findings

Image interpretation sessions were performed in three steps in which two radiologists independently evaluated each patient image for cancer recurrence. In a first preliminary reading phase, each radiologist interpreted T2-weighted images without formulating a judgment of cancer recurrence to avoid a statistical bias, because these images were used during examination execution for VOI positioning. Abnormal tissue localization was determined as follows: periurethral-perianastomotic (circumferential abnormal tissue with low signal compared with the adjacent pelvic muscles on T2-weighted images around bladder-neck and membranous urethra), around the bladder neck, and in the prostatectomy bed. Evaluation was made if the tissue was considered a recurrence or a scar. The major diameter of the suspected tissue was measured and described as circumferential (ie, around the urethra), nodular-like, or plaque-like on a radiological dedicated workstation (Leonardo, Siemens Medical Solutions, Erlangen, Germany).

In the first interpreting session with a different case order, all MR spectra data were overlaid in the three planes (axial, coronal, and sagittal) on the corresponding turbo spin echo (TSE) T2-weighted images, and the following constraints observed: Suspected recurrence tissue was included; urethra, seminal vesicles, ejaculatory ducts, and bladder and rectal wall were excluded; signal-to-noise ratio had to be greater than 3:1; and water/fat suppression had to be adequate. Voxels that did not fit these criteria were considered not useable, as described previously. For each available voxel, the ratio of choline (Cho) plus creatine (Cr) to citrate (Ci) was calculated. On the basis of the literature for 1H-MRSI [21,22], each voxel was categorized as follows: no solid tissue/empty prostatic fossa when Cho + Cr/Ci was undetectable; fibrotic/scar tissue when Cho + Cr/Ci <0.2; residual healthy prostatic gland tissue when Cho + Cr/Ci >0.2 and <0.5; probably recurrent prostate cancer tissue when Cho + Cr/Ci >0.5 and <1; and definitively recurrent prostate cancer tissue when Cho + Cr/Ci >1. Following this analysis, each radiologist formulated an opinion of cancer recurrence.

In the second reading session, cases were evaluated at least 1 mo after the reading of the 1H-MRSI data sets in a different random order, and curves of the following dynamic MR parameters were assessed: onset time (OT); TTP; peak enhancement (PE); washout (WSH). Each reader subjectively and separately evaluated the parametric scale and the parameters in random order, on the basis of the presence,

asymmetry, and degree of enhancement. On the basis of prior studies, we considered early nodular enhancement (prior to enhancement of the rest of the prostatic fossa and pelvic muscles) and early washout to be features that were highly indicative of prostate cancer [23].

Area under the receiver operating characteristic curve (AUC) was calculated to assess which DCEMRI cut-off values were optimal for cancer discrimination in the different patients groups. The readers considered DCEMR images unusable if the time score was not calculable owing to technical problems. Individual assessments of 1H-MRSI and DCEMR were evaluated in conjunction with the T2-weighted images.

The third analysis phase was performed after a further 1 wk delay. In that analysis the same radiologists interpreted the cases including all available data (morphological, 1H-MRSI, and dynamic MRI findings) and formulated a definitive diagnosis. In these patients in whom the result of one method was uncertain compared with that of another method, the radiologists considered imaging findings in complex but had to furnish a definitive judgment however.

2.5. *Histological examination*

All patients were subjected to a TRUS-guided biopsy 5–6 wk after MR imaging of the postprostatectomy fossa, performed with the use of a biplanar 7.5-MHz frequency probe. In patients in whom biochemical relapse emerged, biopsy specimens were taken under TRUS with the use of an 18-G needle loaded in a spring action automatic biopsy device and were fixed overnight in a solution of 10% neutral buffered formalin. TRUS was considered positive if any hypoechoic lesion was identified at the bladder neck or in the retrovesical area, and a correlation with image findings about localization, size, and number of recurrence areas was performed before registration of statistical data. Patients with low PSA elevation and negative TRUS, underwent six random guided biopsies of the prostatic fossa: These patients however were included in the second group of our study.

2.6. *Statistical analysis and clinical validation*

Statistical data analysis was performed with the statistical software MedCalc Software Demo for Windows, version 9.3 (Mariakerke, Belgium). Sensitivities, specificities, positive predictive values (PPVs), negative predictive values (NPVs) of detecting prostate cancer were calculated for the first, second, and third data sets, and receiver operating characteristic (ROC) curves were generated to summarize the data. For the analysis of 1H-MRSI data, a standardized uptake ratio maximum cut-off value of Cho + Cr/Ci >0.5 was employed, and an area under the AUC was calculated to assess which cut-off value for each dynamic curve parameter (OT, TTP, PE, WSH) could be optimal for cancer detection.

Patients were divided into two groups (Table 1) on the basis of the clinical validation used for MR results. The ''gold standard'' for local disease presence was ascertained on the basis of one of the following methods: a reliable TRUS-biopsy result from the postprostatectomy fossa (group A), or a reduction in PSA level (>50%) following radiation therapy (group B). The CG was evaluated as a reference. A patient suspected for local recurrence detected with MR imaging was considered to be true-positive when the imaging results correlated with the conclusive histopathological findings. To allow for reasonable differences in morphology between the evaluated imaging and histopathological findings, we considered the histopathologically and imaging-detected tumors to be of comparable size, localization, and number. When this condition was not respected, a patient was considered to be false-positive. Comparisons of these parameters at per-ROI analysis versus those at per-patient analysis revealed only minor nonsignificant differences.

Table 1 – Patient groups

Group	Patients number[1]	PSA serum level at progression after RRP[2]	Maximal transverse dimension of a mass representing local suspected recurrence[3]	Features and standard validation
A	50 patients (47 with histologic inclusion criteria[4])	0.9 ng/ml–1.9 ng/ml (mean 1.26 ng/ml)	7.6 mm–19.4 mm (mean 13.3 ± 4.5 mm)	Patients in which a TRUS-biopsy of the post-prostatectomy prostatic fossa was performed as control and validation of MR results
B	20 patients	0.4 mg/ml–1.4 ng/ml (mean 0.8 ng/ml)	5.0 mm–7.2 mm (mean 6 ± 0.5 mm)	Patients in which the PSA level modification after radiation therapy was used as validation of MR results
CG	10 patients	No PSA progression (<0.2 ng/ml)		Undetectable PSA serum levels (<0.2 ng/ml) who underwent RRP in the same time interval, as control group (CG)

NOTE: [1]Age range 56 to 72 years (mean 63.8 years), pT3 a-b N0 pathological stage, negative surgical margins, M0; [2] post-RRP PSA increase >0.2 ng/ml from 7 to 20 months after surgery (mean 13 ± 4 months); [3]measured on T2-weighted images; [4]three patients with uncertain TRUS-biopsy findings excluded from the analysis.
CG: control group.

3. Results

Three patients in group A did not have a reliable TRUS biopsy and were therefore excluded from further analysis. In particular these patients had uncertain TRUS biopsy findings, and their MR images demonstrated abundant postsurgical fibrosis, so the demarcation between postsurgical changes and tumor recurrence could not be made. No patients were excluded from group B and CG.

Table 1 summarizes patient characteristics and clinical findings.

3.1. *Group A*

In group A, biopsy-proven local recurrences were identified in 31 of 47 (66%) patients evaluated, whereas 16 (34%) had no biopsy evidence for cancer. PSA level at the time of MR imaging ranged from 0.9 to 1.9 ng/ml (mean, 1.26). The maximal

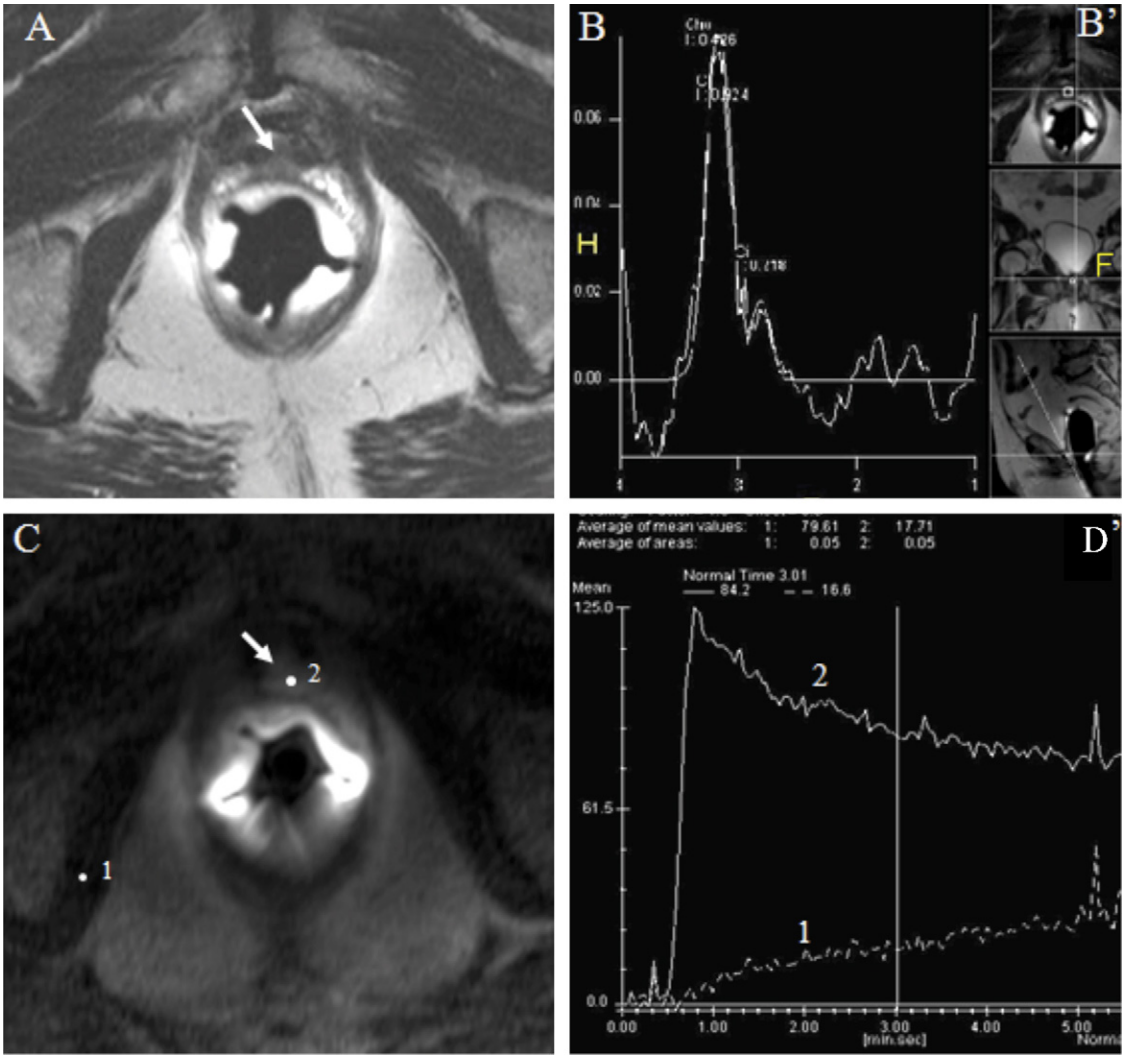

Fig. 1 – Images in a patient with prostate-specific antigen progression after radical prostatectomy, suspected for local recurrence (group A). (A) Transverse T2-weighted fast spin-echo (repetition time (TR), 5190 ms; echo time (TE), 95 ms) magnetic resonance (MR) images show intermediate-signal-intensity mass (arrow) in a periurethral location, suspected for local recurrence, with poor depiction of the borders. (B) B' shows positioning of the volume of interest for MR spectroscopic analysis with three-dimensional chemical shift imaging sequences superimposed on T2-weighted images; in (B), voxel analysis curve shows markedly reduced citrate (Ci) signal and increased choline-creatine to citrate ratio (Cho + Cr/Cit >2) in the area with intermediate signal intensity on T2-weighted images. Three-dimensional fast low-angle shot (FLASH) T1-weighted spoiled gradient-echo image (C) shows a well-defined hypervascular lesion (arrows) relative to the surrounding noncancerous tissue, with excellent depiction of the tumor border. In (D), the corresponding MR signal enhancement-time curve shows a significant difference between pelvic muscle enhancement (region of interest [ROI] 1) and the smaller time to peak and higher peak enhancement values of suspected area (ROI 2). Recurrent carcinoma was histologically validated at transrectal ultrasound-guided biopsy.

Table 2 – MR imaging results for localization of prostate cancer

Imaging modality	Sensitivity	Specificity	PPV	NPV
MR spectroscopic imaging				
Patient group A	84 (26/31)	88 (14/16)	93 (26/28)	74 (14/19)
Patient group B	71 (10/14)	83 (5/6)	91 (10/11)	56 (5/9)
Dynamic MR Imaging				
Patient group A	71 (22/31)	94 (15/16)	96 (22/23)	63 (15(24)
Patient group B	79 (11/14)	100 (6/6)	100 (11/11)	67 (6/9)
Evaluation of combined MRSI and dynamic MR imaging				
Patient group A	87 (27/31)	94 (15/16)	96 (27/28)	79 (15/19)
Patient group B	86 (12/14)	100 (6/6)	100 (12/12)	75 (6/8)

NOTE: Values are expressed in percentage. Number of patients in brackets.
NPV = negative predictive value, PPV = positive predictive value.

transverse dimension of a mass representing local recurrence averaged 13.3 ± 4.5 mm (Fig. 1).

The quality of morphological MR examination was good to excellent in all 47 cases (average signal-to-noise ratio, 3). The location of recurrence within the postprostatectomy fossa was perianastomotic in 13 of 31 patients (41%), around the bladder neck in 11 of 31 (35%), within a retained seminal vesicle in 2 of 31 (6%), and at the anterior or lateral surgical margin in 5 of 31 (16%). Morphology was circumferential in 5 of 31 cases, plaque-like in 8 of 31 cases, and nodular in 18 of 31 cases.

In the independent 1H-MRSI analysis of group A cases (Table 2), spectra consistent with recurrence was correctly observed in 26 of 47 patients; 5 of 47 false-negative, 14 of 47 true-negative, and 2 of 47 false-positive results were observed. The independent DCEMR analysis showed 22 of 47 true-positive with 9 of 47 false-negative, 15 of 47 true-negative, and 1 of 47 false positive cases.

For 1H-MRSI, sensitivity of 84% and specificity of 88% (PPV, 93%; NPV, 74%) were observed. Sensitivity of 71% and specificity of 94% (PPV, 96%; NPV, 63%) were shown for DCEMR (Table 2).

In the combined 1H-MRSI and DCEMR analysis, there were 27 of 47 true-positive, 4 of 47 false-negative, 15 of 47 true-negative, and 1 of 47 false-positive cases. These results yielded a sensitivity of 87% and specificity of 94% (PPV, 96%; NPV, 79%) for the combined 1H- MRSI and DCEMR analysis (Table 2).

The AUCs for 1H-MRSI, DCEMR, and combined 1H-MRSI/DCEMR values were 0.942, 0.931 and 0.964, respectively (standard error [SE], 0.033, 0.036, and 0.026) (Table 3, Fig. 2).

3.2. *Group B*

In group B, a PSA level reduction (>50%) following radiation therapy was observed in 14 of 20 patients

Table 3 – ROC curves and comparison of results

	AUC	Standard error	Difference between areas
First group A: curve A (47 patients)			
1. Spectroscope Evaluation	0.942	0.033	
2. Dynamic Evaluation	0.931	0.036	
3. Combined Spectroscopic and Dynamic Evaluation	0.964	0.026	
First group: pairwise comparison of ROC curves			
1. Spectroscopic versus 2. Dynamic		0.029	0.01
1. Spectroscopic versus 3. Combined SP + DY		0.026	0.022
2. Dynamic versus 3 Combined SP + DY		0.012	0.032
Second group B: curve B (20 patients)			
1. Spectroscopic Evaluation	0.81	0.099	
2. Dynamic Evaluation	0.923	0.061	
3. Combined Spectroscopic and Dynamic Evaluation	0.94	0.053	
Second group: pairwise comparison of ROC curves			
1. Spectroscopic versus 2. Dynamic		0.055	0.113
1. Spectroscopic versus 3. Combined SP + DY		0.06	0.131
2. Dynamic versus 3. Combined SP + DY		0.012	0.018

NOTE: ROC = receiver operating characteristic; DY = Only Dynamic evaluation; SP = Only Spectroscopic evaluation; CI = Confidence Interval.

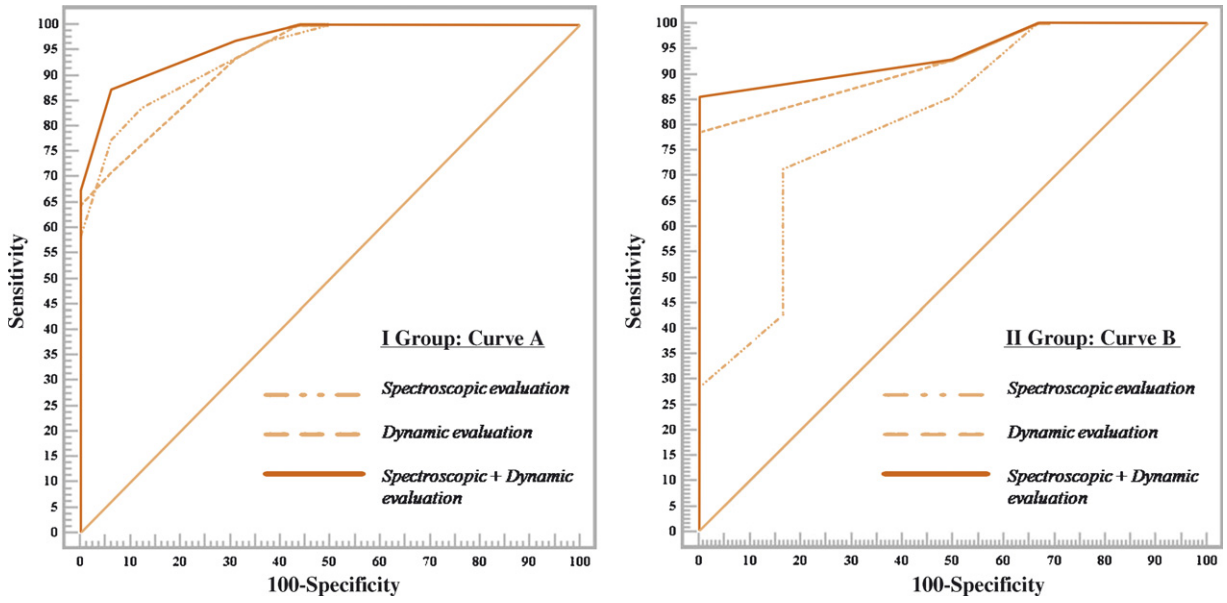

Fig. 2 – Graphs show receiver operating characteristic (ROC) curves comparison for each analysis phase. In (A), ROC curves calculated in the first patient group (group A) show area under the curve (AUC) values for magnetic resonance (MR) spectroscopic imaging (first-phase analysis), dynamic (second-phase analysis), and evaluation of both dynamic and MR spectroscopic imaging (third-phase analysis). AUC was significantly greater in third-phase analysis than with spectroscopic and dynamic imaging, confirming a significantly better performance of the combined MR spectroscopic imaging/dynamic contrast-enhanced MR (1H-MRSI/DCEMR) evaluation of cancer recurrence localization. (1H-MRSI = 0.942 ± SE 0.033, DCEMR = 0.931 ± 0.036. 1H-MRSI + DCEMR = 0.964 ± SE 0.026). In (B), ROC curves calculated in the second patient group (group B) show AUC significantly greater with combined evaluation of both spectroscopic and dynamic findings than with spectroscopic and dynamic imaging alone. In contrast to group A, the spectroscopic evaluation show a lower performance level (a smaller AUC) than dynamic evaluation. Base model included an analysis of choline (Cho) plus creatine (Cr) to citrate (Ci) ratio > 0.5 and < 1 (cut off, ≥0.5) for spectroscopic images and parameters evaluated by different area under the receiver operating characteristic curve (AUC) for DCEMRI. Diagonal line indicates area under ROC curve of 0.500. (1H-MRSI = 0.810 ± SE 0.099, DCEMR = 0.923 ± 0.061, 1H-MRSI + DCEMR = 0.940 ± SE 0.053). See Table 3 for numerical results.

(70%), whereas 6 (30%) had no significant biochemical variations. PSA level at the time of MR imaging ranged from 0.4 to 1.4 ng/ml (mean, 0.8 ng/ml). The mean maximal transverse dimension of a suspected local recurrence was 6 ± 0.5 mm (Fig. 3).

Independent 1H-MRSI showed 10 of 20 true-positive, 4 of 20 false-negative, 5 of 20 true-negative, and 1 of 20 false-positive cases (sensitivity, 71%; specificity, 83%; PPV, 91%; NPV, 56%). Independent DCEMR showed 11 of 20 true-positive, 3 of 20 false-negative, 6 of 20 true-negative, and 0 false-positive cases (sensitivity, 79%; specificity, 100%; PPV, 100%; NPV, 67%). The combined 1H-MRSI/DCEMR showed 12 of 20 true-positive, 2 of 20 false-negative, 6 of 20 true-negative, and 0 false-positive cases (sensitivity, 86%; specificity, 100%; PPV, 100%; NPV, 75%) (Table 2). AUCs were 0.81, 0.923, and 0.94, respectively (SE, 0.099, 0.061, and 0.053) for 1H-MRSI, DCEMR, and combined 1H-MRSI/DCEMR (Table 3, Fig. 2).

3.3. *Control group*

No morphological signs of suspected recurrence were evident in all cases of the CG. Moreover, in all 10 cases, at 1H-MRSI analysis no spectra consistent with recurrence was observed (Cho + Cr/Ci <0.5 in all 10 cases), and at DCEMRI no significant enhancement curves after contrast material injection was described.

4. Discussion

Serial PSA measurements after RP represent the usual follow-up approach for the early detection of prostate cancer recurrence. Clinical nomograms based on PSA or postsurgical pathological parameters have been used to predict whether a recurrence is more likely local or metastatic [7]. Several imaging modalities also have been

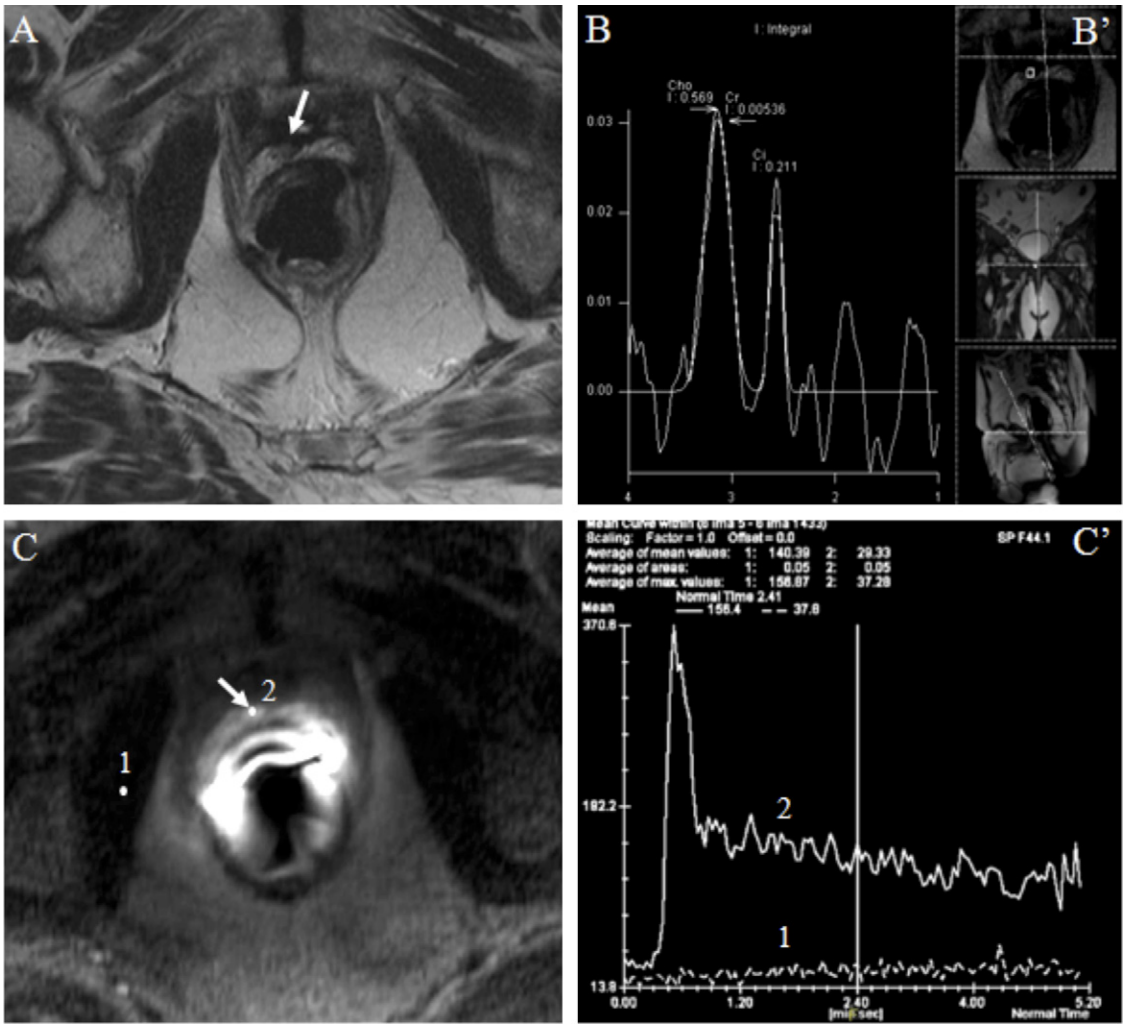

Fig. 3 – Images in a patient with prostate-specific antigen (PSA) progression after radical prostectomy, suspected for local recurrence (group B). (A) Transverse T2-weighted fast spin-echo (repetition time (TR), 5190 ms, echo time (TE), 95 ms) images show a mass of intermediate signal intensity (arrow) in a periurethral location, suspected for local recurrence; (B) B' shows the positioning (with low signal-to-noise ratio) of the volume of interest for magnetic resonance (MR) spectroscopic analysis with three-dimensional (3D) chemical shift imaging sequences on referenced T2-weighted image; in (B), voxel analysis curve show markedly reduced citrate (Ci) signal and increased choline-creatine to citrate ratio (Cho + Cr/Cit = 2.72) (Ci value to be considered as value in the ratio) in an area with intermediate signal intensity on T2-weighted images. 3D fast low-angle shot (FLASH) T1-weighted spoiled gradient-echo image (C) shows a well-defined hypervascular lesion (arrows) relative to the surrounding noncancerous peripheral zone, with excellent depiction of the tumor border. In (C'), the corresponding MR signal enhancement-time curve shows a significant difference between pelvic muscle enhancement (region of interest [ROI] 1) and the smaller time to peak and higher peak enhancement values of suspected area and rapid washout (ROI 2). This finding suggests a local cancer recurrence of 7 mm. In this patient recurrent carcinoma was validated by a PSA serum level decrease after external beam radiotherapy (<0.2 ng/ml).

introduced in the last two decades to support the decision of urologists and oncologists in the therapeutic planning of prostate cancer recurrence: The selection of a technique for prostate cancer recurrence detection should be based on the questions that need to be answered for a particular patient. The imaging protocols are continuously evolving because of changes in clinical care, scientific discoveries, and technological innovations. All three cross-sectional imaging modalities (CT, MR imaging, and US) have been employed in patients with suspected local prostate cancer recurrence, and each have important limitations. TRUS in association with TRUS-guided biopsy is considered the most sensitive modality for the identification of local recurrence [23,24]. It has been shown that TRUS can miss small foci of recurrent prostate cancer at low PSA levels [25], and that the false-negative rate is

15–20% using combined TRUS with prostatic fossa biopsy [26,27]. Leventis et al [28] reported an overall TRUS-guided biopsy detection rate of 41%, and the most consistent achievement of a diagnosis of a local recurrence with TRUS-guided biopsy was in patients with a PSA level higher than 4 ng/ml [28–30]. In our study we separately categorized patients at high risk for local recurrence after RP into two groups: group A, with substantially elevated PSA levels and a feasible TRUS biopsy of the suspected recurrence; and group B, in whom the size of recurrence did not permit a suitable biopsy but all were submitted to radiation therapy. The division into these two groups was established prior to the MR study, and our intention was to separate patients into a first group in whom good accuracy TRUS biopsy results could be expected (group A) and a second group in whom poor TRUS biopsy results may be expected (group B). In our analysis we looked at the accuracy of 1H-MRSI, DCEMR, and combined 1H-MRSI/DCEMR to assess the contribution of each approach to the correct diagnosis. The results obtained in group A showed that each individual assessment and the combined data all performed well: 0.942, 0.931, and 0.964 AUC values, respectively. In comparison, in the more challenging group B, we observed different results from the three assessments: 0.81, 0.923, and 0.94 AUC values, respectively. The lower performance of 1H-MRSI in group B may reflect the problem that the required voxel size for spectroscopic data is larger than that for DCEMR data, and group B patients would be predicted to have smaller volume diseases. Partial volume effects may be predicted to be more problematic with spectroscopy in the setting of small-volume disease. However it is noteworthy that, also in group B, 1H-MRSI provided important data, as evidenced by the larger AUC value in combined 1H-MRSI/DCEMR data over DCEMR data alone. These findings suggest that there may be a higher diagnostic accuracy of combined 1H-MRSI/DCEMR, in particular for patients with a lower increase of PSA levels and small-volume disease [28].

Our sensitivity and specificity values agree with those reported from other studies, such as the Silverman study [30]. In our opinion, our study has not been biased, as in other analyses, with regard to the small number of patients or to the retrospective inclusion of subjects known to be positive for recurrence. However our findings may be biased by the inclusion of subjects with a pT3 surgical staging, reflecting an increased risk for locoregional cancer recurrence.

Further limitations in our study could be represented by voxel size, effect of saturation bands for 1H-MRSI, and 1.5-T field strength. Futterer et al [31] recently demonstrated that 3D CSI at 3-T allows an increase in spatial, temporal, and spectral resolution in the early diagnosis of prostate cancer In addition, in our analysis the quantification of metabolite levels was relative to other metabolites because absolute quantification has not yet been perfected for the MR spectroscopic method used in the study [17]. We found that metabolite ratio depends on factors that could differ among voxels in the same patient or among patients (eg, the distance of the voxels from the endorectal coil, the magnetic field homogeneity, the T2 relaxation times). It should be recognized that these factors could have introduced bias against 1H-MRSI data for the discrimination between benign/fibrotic tissue and cancer. On the other hand, our study shows that any limitation in 1H-MRSI data may be overcome by combining this information with DCEMR.

Conflicts of interest

The authors have nothing to disclose.

References

[1] Yan Y, Carvalhal GF, Catalona WJ, Young JD. Primary treatment choices for men with clinically localized prostate carcinoma detected by screening. Cancer 2000;88:1122–30.

[2] Sakai I, Harada K, Kurahashi T, et al. Usefulness of the nadir value of serum prostate-specific antigen measured by an ultrasensitive assay as a predictor of biochemical recurrence after radical prostatectomy for clinically localized prostate cancer. Urol Int 2006;76:227–31.

[3] Freedland SJ, Sutter ME, Dorey F, Aronson WJ. Defining the ideal cutpoint for determining PSA recurrence after radical prostatectomy. Urology 2003;61:365–9.

[4] Amling CL, Bergstralh EJ, Blute ML, Slezak A, Zincke H. Defining prostate specific antigen progression after radical prostatectomy: what is the most appropriate cutpoint? J Urol 2001;165:1146.

[5] Neulander EZ, Soloway MS. Failure after radical prostatectomy. Urology 2003;61:30–6.

[6] Aus G, Abbou CC, Bolla M, et al. EAU guidelines on prostate cancer. Eur Urol 2005;48:546–51.

[7] Pound CR, Partin AW, Eisenberger MA, Chan DW, Pearson JD, Walsh PC. Natural history of progression after PSA elevation following radical prostatectomy. JAMA 1999;281:1591–7.

[8] Kramer S, Gorich J, Gottfried HW, et al. Sensitivity of computed tomography in detecting local recurrence of prostatic carcinoma following radical prostatectomy. Br J Radiol 1997;70:995–9.

[9] Raj GV, Partin AW, Polascik TJ. Clinical utility of indium 111-capromab pendetide Immunoscintigraphy in the detection of early, recurrent prostate carcinoma after radical prostatectomy. Cancer 2002;94:987–96.
[10] Hara T, Kosaka N, Kishi H. PET imaging of prostate cancer using carbon-11- choline. J Nucl Med 1998;39:990–5.
[11] Scattoni V, Montorsi F, Picchio M, et al. Diagnosis of local recurrence after radical prostatectomy. BJU Int 2004;93: 680–8.
[12] Saleem MD, Sanders H, El Naser MA. Factors predicting cancer in biopsy of the prostatic fossa after radical prostatectomy. Urology 1998;51:283–6.
[13] Connolly JA, Shinohara K, Presti Jr JC. Local recurrence after radical prostatectomy: characteristics in size, location, and relationship to prostate-specific antigen and surgical margins. Urology 1996;47:225–31.
[14] Anastasiadis AG, Lichy MP, Nagele U, et al. MRI-guided biopsy of the prostate increases diagnostic performance in men with elevated or increasing PSA levels after previous negative TRUS biopsies. Eur Urol 2006;50:738–49.
[15] Forman JD, Meetze K, Pontes E. Therapeutic irradiation for patients with an elevated post-prostatectomy prostate specific antigen level. J Urol 1997;158:1436–9.
[16] Miralbell R, Vees H, Lozano J, et al. Endorectal MRI assessment of local relapse after surgery for prostate cancer: a model to define treatment field guidelines for adjuvant radiotherapy in patients at high risk for local failure. Int J Radiat Oncol Biol Phys 2007;67:356–61.
[17] Hricak H, Choyke PL, Eberhardt SC, Leibel SA, Scardino PT. Imaging prostate cancer: a multidisciplinary perspective [review]. Radiology 2007;243:28–53.
[18] Pucar D, Koutcher JA, Shah A, et al. Preliminary assessment of magnetic resonance spectroscopic imaging in predicting treatment outcome in patients with prostate cancer at high risk for relapse. Clin Prostate Cancer 2004;3:174–81.
[19] Hricak H, Schoder H, Pucar D, et al. Advances in imaging in the postoperative patient with a rising prostate-specific antigen level. Semin Oncol 2003;30:616–34.
[20] Amsellem-Ouazana D, Younes P, Conquy S, et al. Negative prostatic biopsies in patients with a high risk of prostate cancer: is the combination of endorectal MRI and magnetic resonance spectroscopy imaging (MRSI) a useful tool? A preliminary study. Eur Urol 2005;47:582–6.
[21] Perrotti M, Han KR, Epstein RE, et al. Prospective evaluation of endorectal magnetic resonance imaging to detect tumor foci in men with prior negative prostastic biopsy: a pilot study. J Urol 1999;162:1314–7.
[22] Kirkham APS, Emberton M, Allen C. How good is MRI at detecting and characterising cancer within the prostate? Eur Urol 2006;50:1163–75.
[23] Prando A, Kurhanewicz J, Borges AP, Oliveira Jr EM, Figueiredo E. Prostatic biopsy directed with endorectal MR spectroscopic imaging findings in patients with elevated prostate specific antigen levels and prior negative biopsy findings: early experience. Radiology 2005;236:903–10.
[24] Futterer JJ, Heijmink SW, Scheenen TW, et al. Prostate cancer localization with dynamic contrast-enhanced MR imaging and proton MR spectroscopic imaging. Radiology 2006;241:449–58.
[25] Nash PA, Bruce JE, Indudhara R. Transrectal ultrasound guided prostatic nerve blockade eases systematic needle biopsy of the prostate. J Urol 1996;155:607–9.
[26] Parra RO, Wolf RM, Huben RP. The use of transrectal ultrasound in the detection and evaluation of local pelvic recurrence after a radical urological pelvic operation. J Urol 1990;144:707–9.
[27] Leventis AK, Shariat SF, Slawin KM. Local recurrence after radical prostatectomy: correlation of US features with prostatic fossa biopsy findings. Radiology 2001;219:432–9.
[28] Shekarriz B, Upadhyay J, Wood Jr DP. Vesicourethral anastomosis biopsy after radical prostatectomy: predictive value of prostate-specific antigen and pathologic stage. Urology 1999;54:1044–8.
[29] Deliveliotis C, Manousakas T, Chrisofos M, Skolarikos A, Delis A, Dimopoulos C. Diagnostic efficacy of transrectal ultrasound-guided biopsy of the prostatic fossa in patients with rising PSA following radical prostatectomy. World J Urol 2007;25:309–13.
[30] Silverman JM, Krebs TL. MR imaging evaluation with a transrectal surface coil of local recurrence of prostatic cancer in men who have undergone radical prostatectomy. AJR Am J Roentgenol 1997;168:379–85.
[31] Futterer JJ, Scheenen TW, Huisman HJ, et al. Initial experience of 3 Tesla endorectal coil magnetic resonance imaging and 1H-spectroscopic imaging of the prostate. Invest Radiol 2004;39:671–80.

Editorial Comment on: Role of Dynamic Contrast-Enhanced Magnetic Resonance (MR) Imaging and Proton MR Spectroscopic Imaging in the Detection of Local Recurrence after Radical Prostatectomy for Prostate Cancer

Noboru Hara
Division of Urology, Department of Regenerative and Transplant Medicine, Graduate School of Medical and Dental Sciences, Niigata University, Niigata 951-8510, Japan
harasho@med.niigata-u.ac.jp
noboharasho@par.odn.ne.jp

Despite recent advances in diagnostic and surgical techniques, prostate-specific antigen (PSA)-based recurrence of prostate cancer after radical prostatectomy (RP) has been reported to range between 15% and 20% [1]. For men with prostate cancer indicated for radical treatments, however, RP is expected to remain the therapeutic mainstay for the foreseeable future, because it is the sole window through which we can accurately determine the pathologic condition of the disease. PSA failure is an initial criterion for local recurrence or metastasis in men with prostate

cancer who have undergone radical treatments. It is frequently difficult to distinguish between these recurrence patterns by PSA-based monitoring alone, but distinguishing these patterns is important for selecting the appropriate salvage option [3]. Accordingly, improvement in localizing the diagnosis for prostate cancer recurrence during an earlier postoperative period is a challenging problem. The present report by Sciarra et al showed that combined dynamic contrast-enhanced magnetic resonance imaging (MRI) and 1H-spectroscopic imaging are promising modalities to identify and visualize recurrent lesions for patients under such situations [2]. To our knowledge, this is the first study that enrolled a statistically sufficient number of patients and demonstrated the practical utility of MRI for the detection of locally recurrent prostate cancer following surgery. Furthermore, the current study took a characteristic and subtle approach by setting double criteria for assessing the usefulness of MRI; one trial group was comprised of cases evaluated by transrectal ultrasonography-guided biopsy and the other arm was assessed by the outcome following salvage radiotherapy, thereby overcoming a common limitation in this type of study where the findings largely depend on the biopsy technique [4]. Treatment selection in patients with postprostatectomy recurrence is an issue of general concern [5], and the present findings may influence the approaches of future clinical trials focusing on the management of postoperative prostate cancer recurrence.

References

[1] Porter CR, Gallina A, Kodama K, et al. Prostate cancer-specific survival in men treated with hormonal therapy after failure of radical prostatectomy. Eur Urol 2007;52:446–54.
[2] Sciarra A, Panebianco V, Di Silverio F, et al. Role of dynamic contrast-enhanced magnetic resonance (MR) imaging and proton MR spectroscopic imaging in the detection of local recurrence after radical prostatectomy for prostate cancer. Eur Urol 2008;54:589–600.
[3] Gronau E, Goppelt M, Harzmann R, Weckermann D. Prostate cancer relapse after therapy with curative intention: a diagnostic and therapeutic dilemma. Onkologie 2005;28:361–6.
[4] Deliveliotis C, Manousakas T, Chrisofos M, Skolarikos A, Delis A, Dimopoulos C. Diagnostic efficacy of transrectal ultrasound-guided biopsy of the prostatic fossa in patients with rising PSA following radical prostatectomy. World J Urol 2007;25:309–13.
[5] Swanson GP, Hussey MA, Tangen CM, et al., SWOG 8794. Predominant treatment failure in postprostatectomy patients is local: analysis of patterns of treatment failure in SWOG 8794. J Clin Oncol 2007;25:2225–9.

DOI: 10.1016/j.eururo.2007.12.035

DOI of original article: 10.1016/j.eururo.2007.12.034

Editorial Comment on: Role of Dynamic Contrast-Enhanced Magnetic Resonance (MR) Imaging and Proton MR Spectroscopic Imaging in the Detection of Local Recurrence after Radical Prostatectomy for Prostate Cancer

Jurgen J. Fütterer, Jelle O. Barentsz
Department of Radiology,
Radboud University Nijmegen Medical Centre,
Nijmegen, The Netherlands
J.Futterer@rad.umcn.nl

Functional magnetic resonance imaging (MRI) techniques are increasingly used in patients with prostate cancer. These techniques include proton MR spectroscopic imaging (MRSI), dynamic contrast-enhanced MRI (DCEMRI), and diffusion-weighted MRI. In recent years, literature data have shown that the combination of these functional imaging techniques represents an adequate tool for localizing the tumor in the untreated prostate [1,2].

Sciarra et al report on the use of DCEMRI and MRSI in the detection of local recurrence in patients after prostatectomy [3]. The study is based on data from a series of 70 patients at a single institution. The authors assessed and compared the accuracies of these functional imaging tools in detecting local recurrence. They concluded that the combination of DCEMRI and MRSI is an accurate method to identify local prostate cancer recurrence with biochemical failure. This combination resulted in 87% sensitivity and 94% specificity.

After radical prostatectomy, patients are generally followed up by means of digital rectal examination and measurements of the prostate-specific antigen level. Because biochemical failure is not equivalent to clinical failure and may represent isolated local recurrence, systemic recurrence, or both, management of these patients is controversial. Local control is usually assessed

with transrectal ultrasound-guided biopsy [4], but this is invasive and has limited accuracy after radiation. Furthermore, the traditional strategy of waiting until patients develop biochemical or clinical recurrence before initiating salvage therapy has been questioned.

DCEMRI and MRSI after prostatectomy or radiation therapy are clearly options to detect or rule out local recurrence in patients with biochemical failure. The presence or absence of persistent cancer at needle biopsy performed 2 yr after radiation has been established as an important predictor of long-term outcome [5]. Ultimately, MRI could facilitate early detection and might allow for earlier salvage therapy and better long-term outcomes. These functional MRI techniques can also be applied to localize prostate cancer in the untreated prostate. For example, accurate cancer location with regard to the neurovascular bundle is important for the urologist in case of a nerve-sparing radical prostatectomy.

I believe that use of (functional) MRI of the prostate is extremely important in patient management and that urologists should increasingly consider this imaging modality in their decision-making process.

References

[1] Kurhanewicz J, Vigneron DB, Hricak H, Narayan P, Carroll P, Nelson SJ. Three-dimensional H-1 MR spectroscopic imaging of the in situ human prostate with high (0.24–0.7-cm^3) spatial resolution. Radiology 1996;198:795–805.

[2] Fütterer JJ, Heijmink SW, Scheenen TW, et al. Prostate cancer localization with dynamic contrast-enhanced MR imaging and proton MR spectroscopic imaging. Radiology 2006;241:449–58.

[3] Sciarra A, Panebianco V, Di Silverio F, et al. Role of dynamic contrast-enhanced magnetic resonance (MR) imaging and proton MR spectroscopic imaging in the detection of local recurrence after radical prostatectomy for prostate cancer. Eur Urol 2008;54:589–600.

[4] Scattoni V, Montorsi F, Picchio M, et al. Diagnosis of local recurrence after radical prostatectomy. BJU Int 2004;93:680–8.

[5] Pollack A, Zagars GK, Antolak JA, Kuban DA, Rosen II. Prostate biopsy status and PSA nadir level as early surrogates for treatment failure: analysis of a prostate cancer randomized radiation dose escalation trial. Int J Radiat Oncol Biol Phys 2002;54:677–85.

DOI: 10.1016/j.eururo.2007.12.036

DOI of original article: 10.1016/j.eururo.2007.12.034